



Variability of Bering Sea eddies and primary productivity along the shelf edge during 1998–2000 using satellite multisensor remote sensing

Kohei Mizobata*, Sei-ichi Saitoh

Laboratory of Marine Environment and Resource Sensing, Graduate School of Fisheries Sciences, Hokkaido University, 3-1-1, Minato-cho, Hakodate 041-8611, Japan

Received 21 February 2003; accepted 25 September 2003
Available online 19 May 2004

Abstract

TOPEX/Poseidon sea surface height anomalies (SSHAs), Sea-viewing Wide Field-of-view Sensor (SeaWiFS) L3 chlorophyll *a* (chl-*a*) concentration, and primary production were examined to determine the relationship between an eddy field and primary productivity along the shelf edge in the southeastern Bering Sea. Primary production was calculated from SeaWiFS chl-*a*, photosynthetically active radiation (PAR), and AVHRR sea surface temperature (SST) data using the vertically generalized production model (VGPM).

A time–latitude plot of SSHAs, which was derived from TOPEX/Poseidon ground track D-79 along the shelf edge, described the northwestward propagation of positive SSHAs (indicating an anticyclonic eddy) and negative SSHAs (indicating a cyclonic eddy staying near Zhemchug Canyon or over the deep basin). There were increases in the variability of the SSHA field and the speed of eddy propagation during 2000 along the shelf edge. Time–latitude plots of SeaWiFS chl-*a* exhibited relatively high chl-*a* (over 1.0 mg m^{-3}) along the shelf edge for 2–3 months in the summer of 1999, when there was low eddy activity, and for about 6 months in 2000, when there was an eddy-rich environment. The same pattern of chl-*a* appeared in time–latitude plots of primary production. Monthly averaged primary production along the shelf edge was 20.88, 18.37, and $24.04 \text{ g C m}^{-2} \text{ month}^{-1}$ in 1998, 1999, and 2000, respectively. Primary production decreased from about $28 \text{ g C m}^{-2} \text{ month}^{-1}$ (June) to about $18 \text{ g C m}^{-2} \text{ month}^{-1}$ (July) in 1999; however, about $25 \text{ g C m}^{-2} \text{ month}^{-1}$ of primary production was maintained from June to September in 2000. These results indicate a positive correlation between the variability in the Bering Slope Current (BSC) eddy field and primary production along the Bering Sea shelf edge. An increase in the BSC transport and the eddy field fluctuation contributed to the vertical nutrient supply to the subsurface layer and shelf–slope exchange, thereby maintaining high primary productivity along the shelf edge of the southeastern Bering Sea in 2000.

© 2004 Elsevier B.V. All rights reserved.

Keywords: Bering Sea eddy; Shelf edge; TOPEX/Poseidon; SeaWiFS; Primary production; Topographic effects

* Corresponding author.

E-mail address: mizobata@salmon.fish.hokudai.ac.jp (K. Mizobata).

1. Introduction

The Bering Sea shelf break is a part of the boundary that forms the cyclonic Bering Sea gyre (Fig. 1). Along the shelf break, the Bering Slope Current (BSC), the eastern boundary current of Bering Sea gyre, flows at about $5\text{--}15\text{ cm s}^{-1}$ northwestward and commonly forms mesoscale eddies (Kinder et al., 1975, 1980; Schumacher and Reed, 1992; Stabeno and Reed, 1994; Schumacher and Stabeno, 1994; Cokelet and Stabeno, 1997; Mizobata et al., 2002). The structures of the BSC show either a highly variable flow interspersed with eddies, meanders, and instabilities, or a regular northwestward-flowing current (Stabeno et al., 1999). These eddies are ubiquitous features in the oceanic region of the Bering Sea (Schumacher and Stabeno, 1994; Napp et al., 2000) and can be detected by satellite altimeter

throughout the year (Okkonen, 1993, 2001). Recently, several studies have shown there is an onshelf flow associated with mesoscale eddies from the oceanic region to the shelf region (Schumacher and Reed, 1992; Schumacher and Stabeno, 1994; Stabeno and Meurs, 1999). These onshelf flow and eddy movement indicate that exchange occurs between the shelf and the slope. This exchange is thought to be an important process for maintaining the high productivity of the “Green Belt” (Springer et al., 1996; Stabeno et al., 1999; McRoy et al., 2001).

The biological, chemical, and physical structures of Bering Sea eddies have already been observed (Sapozhnikov, 1993; Cokelet and Stabeno, 1997; Mizobata et al., 2002) and the effects of these eddies on nitrogen and phytoplankton distributions have been described. Rising isopycnals indicate that nutrient-rich water is upwelled to the euphotic zone,

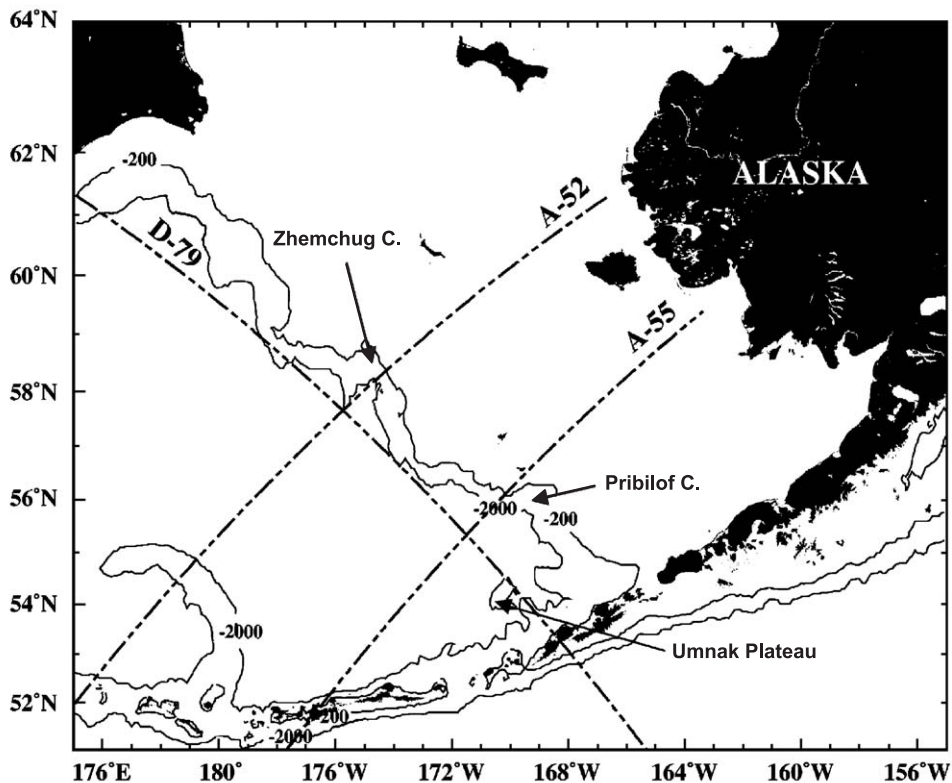


Fig. 1. The Bering Sea shelf edge shown by the 200- and 2000-m isobaths and TOPEX/Poseidon ground tracks D-79, A-52, and A-55 (dotted line) are shown. Complex shelf edge features includes Zhemchug Canon and Pribilof Canyon.

leading to relatively high chlorophyll *a* (chl-*a*) concentrations ($>1.0 \text{ mg m}^{-3}$) at the center of cyclonic eddy and around the periphery of the anticyclonic eddy (Mizobata et al., 2002). The downwelling of the surface warm water with low nutrients destroyed a cold layer resulting from winter convection at the center of the anticyclonic eddy. These eddies have been shown to influence both lower and higher trophic levels, especially walleye pollock *Theragra chalcogramma* (Incze et al., 1991; Schumacher and Stabeno, 1994; Schumacher et al., 1993; Bograd et al., 1994; Napp et al., 2000). In the Bering Sea basin, data from satellite-tracked drifters indicate that high concentrations of larval pollock are associated with eddies (Schumacher and Stabeno, 1994). Despite the importance of these eddies, their horizontal distribution and motion in the oceanic region are still unknown. In this study, we analyzed satellite altimeter and chl-*a* data to understand the relationship between the Bering Slope Current eddy field and the primary production along the Bering Sea shelf edge.

2. Data and methods

2.1. TOPEX/Poseidon sea surface height anomaly (SSHA)

The Bering Slope Current eddy field can be described using TOPEX/Poseidon SSHAs (Okkonen, 2001). In this study, SSHAs were calculated from TOPEX/Poseidon Merged Geophysical Data Record Generation-B from January 1998 to December 2000 (cycle 195–305) distributed by the NASA/Jet Propulsion Laboratory PO.DAAC (Benada, 1997). We examined TOPEX/Poseidon ground track D-79 (54°N–60.5°N), A-52 (180°E–174°W), and A-55 (175°W–170°W) SSHAs to reveal the variability and movement of the Bering Slope Current eddy field (Fig. 1). Then the root mean square (RMS) of SSHAs along D-79 was estimated to illustrate eddy activity along the shelf edge.

2.2. SeaWiFS sea surface chl-*a*

Sea surface chl-*a* (mg m^{-3}) obtained by satellite ocean color sensors often showed mesoscale fea-

tures (Fig. 2). Monthly Sea-viewing Wide Field-of-view Sensor (SeaWiFS) Level 3 chl-*a* standard mapped images with 9 km of spatial resolution (OC4V4; January 1998–December 2000) were processed for comparison with the SSHAs data. After Mercator mapping using the SeaWiFS Data Analysis System (SeaDAS) distributed by NASA Goddard Space Flight Center, 5×5 pixel ($45 \times 45 \text{ km}$) averaged chl-*a* values were extracted directly under the TOPEX/Poseidon orbital ground track D-79 to exclude cloud effects caused by the substantial cloud cover in the Bering Sea. In this study, we used this averaged value to focus on the effect of the mesoscale eddies (diameter = 50–200 km). Smaller eddies (diameter $< 50 \text{ km}$) were excluded from the analyses.

2.3. Primary production

Primary Production (PP_{eu}) was calculated from SeaWiFS Level 3 chl-*a*, SeaWiFS Level 3 photosynthetically active radiation (PAR; mol quanta m^{-2}), and NOAA/AVHRR Oceans Pathfinder sea surface temperature (SST) data (October 1997–May 2001) using the vertically generalized production model (VGPM) developed by Behrenfeld and Falkowski (1997) (hereafter referred to as BF97) and improved by Kameda and Ishizaka (2004) (hereafter referred to as KI02). Both SeaWiFS Level 3 PAR and AVHRR SST have a 9-km resolution, as does SeaWiFS Level 3 chl-*a*. The VGPM can estimate the PP_{eu} ($\text{mg C m}^{-2} \text{ day}^{-1}$) derived from the relationship between surface chlorophyll and depth-integrated primary production. A detailed description of the VGPM is presented in BF97, so a brief overview is given here. The main equation is expressed as:

$$\text{PP}_{\text{eu}} = \text{Chl}_{\text{surf}} Z_{\text{eu}} P_{\text{opt}}^{\text{B}} \text{DL} \left[0.66125 \frac{E_0}{E_0 + 4.1} \right] \quad (1)$$

where Chl_{surf} is the SeaWiFS chl-*a* described previously, DL is daylength (or photoperiod) in decimal hours, Z_{eu} is the physical depth of the euphotic zone defined as the penetration depth of 1% of surface irradiance and calculated from Chl_{surf} , and E_0 is

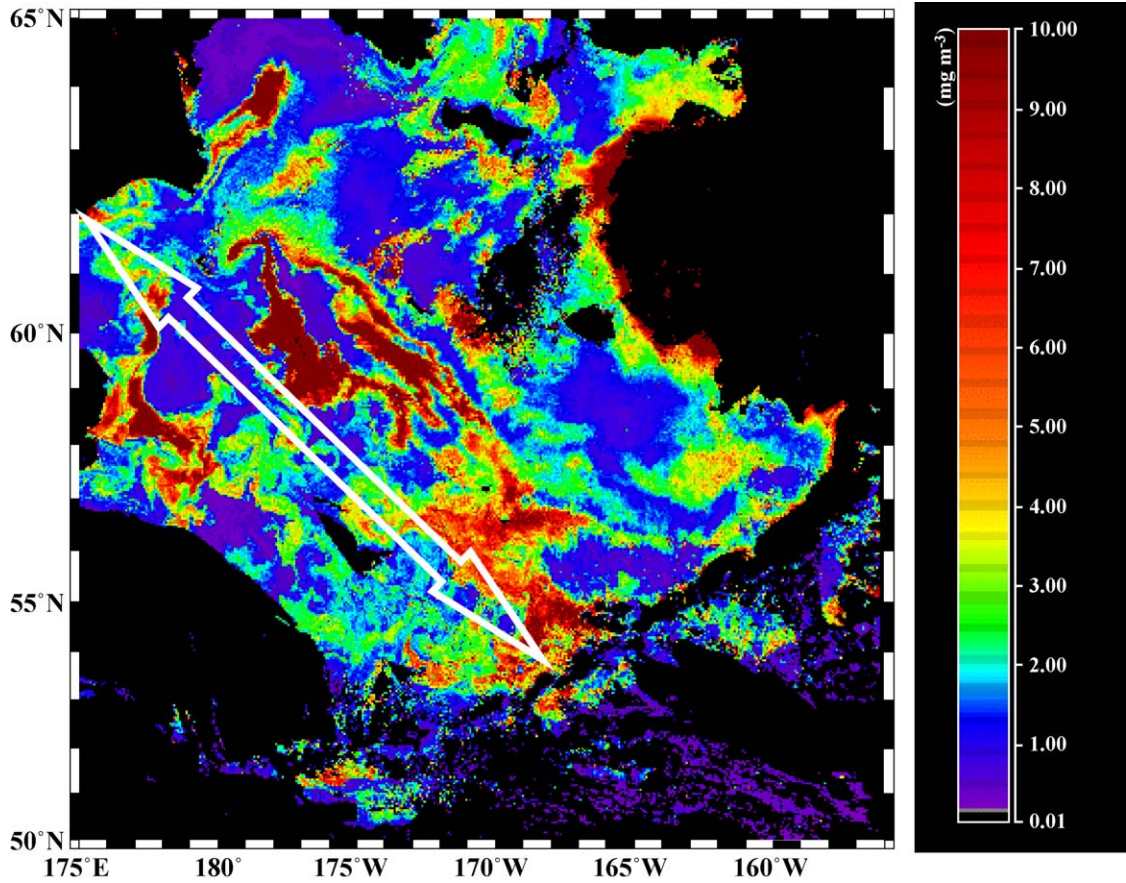


Fig. 2. SeaWiFS chl-*a* composite image of the Bering Sea basin in May and June 2001. In the shelf region and deep basin, chl-*a* concentrations were low. Along the shelf edge (white arrow), however, there were high chl-*a* ring (54°N, 167°W) and bands associated with many mesoscale features, indicating the “Green Belt.”

SeaWiFS Level 3 PAR. The bracketed equation is called the F function, which is the relative fraction of potential photosynthesis lost within the euphotic zone due to light limitation.

$P_{\text{opt}}^{\text{B}}$ in Eq. (1) is the optimal rate of daily carbon fixation within the water column [$\text{mg C (mg Chl)}^{-1} \text{ hour}^{-1}$]. BF97 described $P_{\text{opt}}^{\text{B}}$ as:

$$P_{\text{opt}}^{\text{B}} = \begin{cases} 1.13 & \text{if } T < -1.0 \\ 4.00 & \text{if } T > 28.5 \\ P_{\text{opt}}^{\text{B}'} & \text{otherwise} \end{cases} \quad (2)$$

$$P_{\text{opt}}^{\text{B}'} = 1.2956 + 2.749 \times 10^{-1}T + 6.17 \times 10^{-2}T^2 - 2.05 \times 10^{-2}T^3 + 2.462 \times 10^{-3}T^4 - 1.348 \times 10^{-4}T^5 + 3.4132 \times 10^{-6}T^6 - 3.27 \times 10^{-8}T^7 \quad (3)$$

where T is SST ($^{\circ}\text{C}$). KI02 showed that the BF97 VGPM with its high variance of $P_{\text{opt}}^{\text{B}}$ tends to overestimate or underestimate PP_{eu} at high or low chl-*a* areas in the North Pacific and Japan Sea, respectively. Moreover, KI02 found a relationship among $P_{\text{opt}}^{\text{B}}$, SST, and Chl_{tot} from their in situ database in the North Pacific. Several studies have shown that various sizes and species of phytoplankton occur at the Bering

Sea shelf edge and in the Bering Sea Basin, including microphytoplankton, nanophytoplankton, and picophytoplankton (Sukahanova et al., 1999; Shiimoto et al., 2002; Liu et al., 2002). Then KI02 suggested a new $P_{\text{opt}}^{\text{B}}$ in consideration of a dual phytoplankton (large and small size) community as:

$$P_{\text{opt}}^{\text{B}} = (0.071T - 3.2 \times 10^{-3}T^2 + 3.0 \times 10^{-5}T^3) / \text{Chl}_{\text{surf}} + (1.0 + 0.17T - 2.5 \times 10^{-3}T^2 - 8.0 \times 10^{-5}T^3) \quad (4)$$

where T is the NOAA/AVHRR Pathfinder SST data described before. In this study, we used the VGPM with the KI02 $P_{\text{opt}}^{\text{B}}$ to estimate the primary production along the shelf edge.

3. Results

3.1. Bering Slope Current eddy field in the summer of 1998–2000

The TOPEX/Poseidon orbital ground track D-79 lies along the shelf edge of the Bering Sea (Fig. 1). Following Okkonen (2001), time–latitude plots of SSHAs (Fig. 3a) were used in this study. Fig. 3a shows the characteristics of SSHA variability along and across the shelf edge. The distribution of positive and negative SSHAs is roughly separated from 54°N to 56°N and from 56.5°N to 60.5°N in 1998 (before cycle 230). After cycle 230, however, this separation was unclear. Separation of the BSC has been inferred from drifter trajectories and altimeter analyses (Stabenroed and Reed, 1994; Okkonen, 2001) and is probably due to the tongue-like shape of the shelf break between Zhemchug Canyon and Pribilof Canyon. While most of the positive SSHAs, which indicate anticyclonic eddies, propagated northwestwardly along the shelf edge over Umnak Plateau from 55°N to 56°N, the negative SSHAs, which indicate cyclonic eddies, tended to remain over the Umnak Plateau and near Zhemchug Canyon and did not move. Positive SSHAs in 1998 and 1999 continued for longer periods (about 5–6 months) than in 2000 (about 2–4 months). The averaged velocity of eddy propagation along D-79 was 1.40 cm s⁻¹ in 1998 and

0.79 cm s⁻¹ in 1999 with a standard error of 0.36 and 0.43 cm s⁻¹, respectively. In 2000, however, this velocity was 2.26 cm s⁻¹ with a standard error of 0.46 cm s⁻¹. The D-79 SSHAs RMS had high (RMS=60–200 mm) and low (RMS=20–60 mm) variability in the summers of 1998 and 1999, respectively (Fig. 3b). Beginning in January 2000, this variability shifted from a relatively stable mode to an unstable mode, and the gradient of positive SSHAs propagation became steep.

The ground tracks of A-52 and A-55 lie across the continental slope around Zhemchug Canyon and near the Pribilof Islands, respectively (Fig. 1). Time–longitude plots of the SSHAs show an offshore propagation of both anticyclonic and cyclonic eddies previously described by Okkonen (2001) or retention in the vicinity of continental slope, but there is little indication of SSHAs or eddies moved onto the shelf (Fig. 4a and b).

3.2. Chl-*a* concentration and primary production along the Green Belt

We estimated chl-*a* and primary production directly under TOPEX/Poseidon ground track D-79 and then compared these biological datasets to the eddy field derived from the TOPEX/Poseidon SSHAs. Time–latitude plots of chl-*a* and primary production are shown in Fig. 5a and b. No SeaWiFS chl-*a* data were obtained from 59.5°N to 60.5°N due to the cloud cover. The distribution and duration of relatively high chl-*a* (>1.0 mg m⁻³) and primary production (20 g C m⁻² month⁻¹) fluctuated along the shelf edge from April to October each year. High chl-*a* concentrations, indicative of the spring bloom along the shelf edge, were observed in May 1998, June 1999, and June 2000. However, it is notable that chl-*a* and primary production from 55.5°N to 59.5°N continued only 2–3 months in the summer of 1999 when low eddy activity was described in previous altimeter analyses. Conversely, high chl-*a* and primary production persisted about 6 months after the spring bloom in 2000. Over the Umnak Plateau, from 54°N to 55.5°N, relatively high chl-*a* and primary production were maintained for 4–6 months in 1998, 1999, and 2000.

Averaged primary production along the shelf edge is well reflected in the fluctuation of the productivity

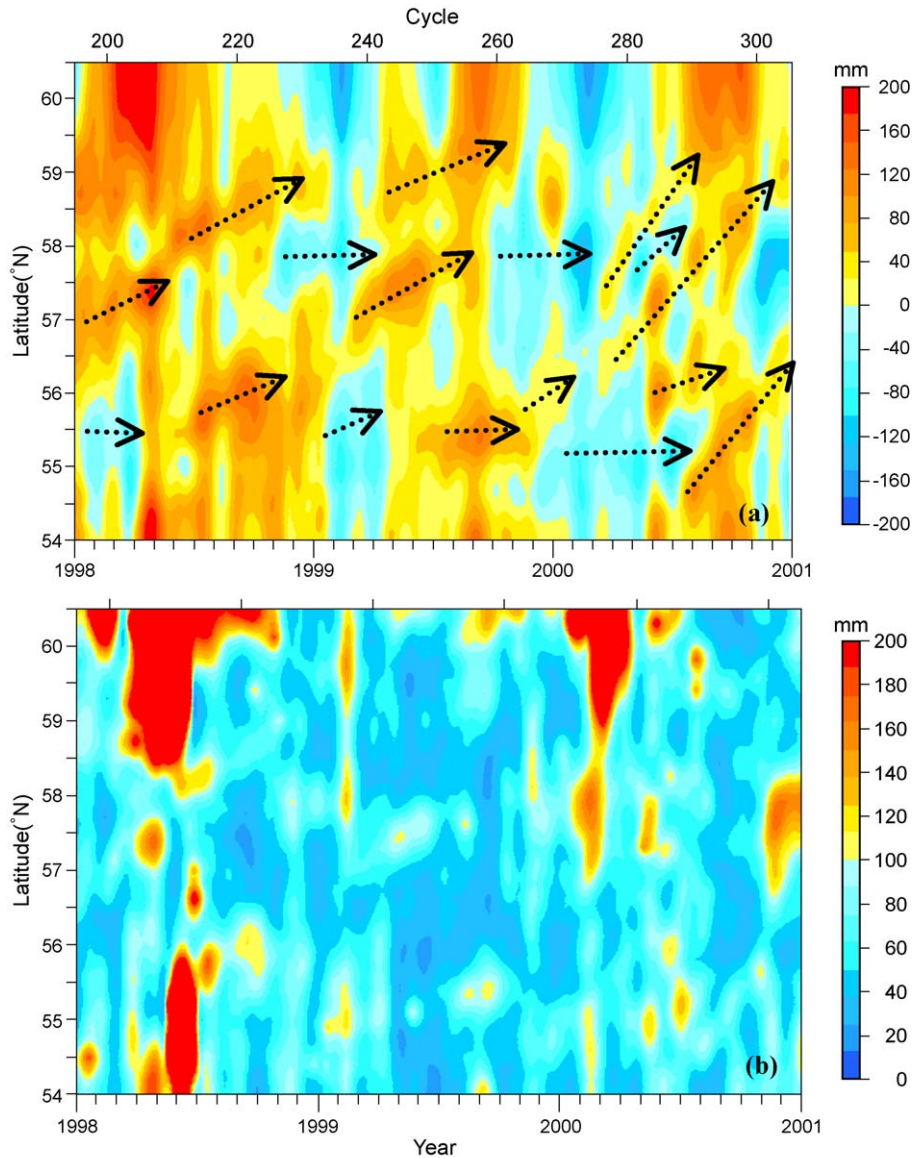


Fig. 3. Time–latitude plot of (a) TOPEX/Poseidon D-79 SSHAs and (b) SSHAs root mean square. Arrows show the direction of eddy propagation.

(Fig. 6). Averaged primary production along the shelf edge decreased from about $28 \text{ g C m}^{-2} \text{ month}^{-1}$ in June to about $18 \text{ g C m}^{-2} \text{ month}^{-1}$ in July of 1999. In 2000, however, more than $25 \text{ g C m}^{-2} \text{ month}^{-1}$ of primary production was maintained from June to September. Monthly averaged primary production along the shelf edge was $20.88 \text{ g C m}^{-2} \text{ month}^{-1}$ in 1998, $18.37 \text{ g C m}^{-2} \text{ month}^{-1}$ in 1999, and 24.04

$\text{g C m}^{-2} \text{ month}^{-1}$ in 2000 with a standard error of 3.48, 3.00, and $3.49 \text{ g C m}^{-2} \text{ month}^{-1}$, respectively.

4. Discussion

Isopleths of SSHAs described the difference in behavior between cyclonic eddies and anticyclonic

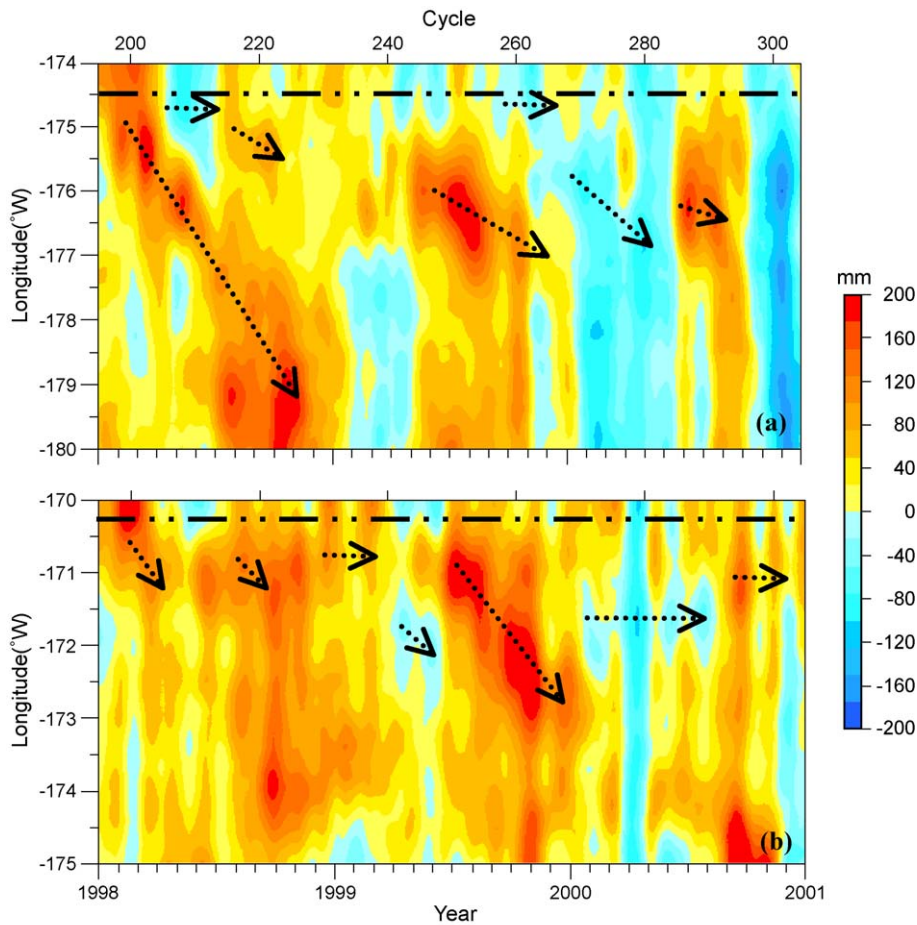


Fig. 4. Time–longitude plot of SSHAs using TOPEX/Poseidon ground tracks (a) A-52 and (b) A-55. Dotted line represented the shelf break at the 2000-m isobath. Arrows show the direction of eddy propagation.

eddies. Along the shelf edge of the Bering Sea, TOPEX/Poseidon-positive SSHAs (anticyclonic eddies) propagated northwestward as described in Okkonen (2001); however, negative SSHAs (cyclonic eddies) tended to remain around the shelf break near Zhemchug Canyon and Pribilof Canyon. Additionally, our analysis showed the BSC eddy field separated at $\sim 56.5^{\circ}\text{N}$ before TOPEX/Poseidon orbital cycle 230. These observations suggest that the continental slope topography affects the BSC eddy field (Stabeno and Reed, 1994; Okkonen, 2001). Certainly, there is another possibility that the TOPEX/Poseidon ground track could not recognize the smaller eddies (<25 km) that slipped offshore.

Movement of an eddy onto the shelf described by Schumacher and Stabeno (1994) was not recognized using TOPEX/Poseidon Ascending tracks 52 and 55 (Fig. 4a and b), but they did show that there are onshelf flows described in previous many studies (Schumacher and Reed, 1992; Schumacher and Stabeno, 1994; Stabeno and Meurs, 1999; Stabeno et al., 1999). Shelf–Slope exchange can occur virtually anywhere along the shelf break (Stabeno et al., 1999) and a SeaWiFS chl-*a* image (Fig. 2) implies that the advection by mesoscale features is important for horizontal mixing. In short, shelf–slope exchange occurred as a result of the advection by a “mesoscale eddy chain” along the shelf break rather than the onshore migration of eddies. Although Schumacher

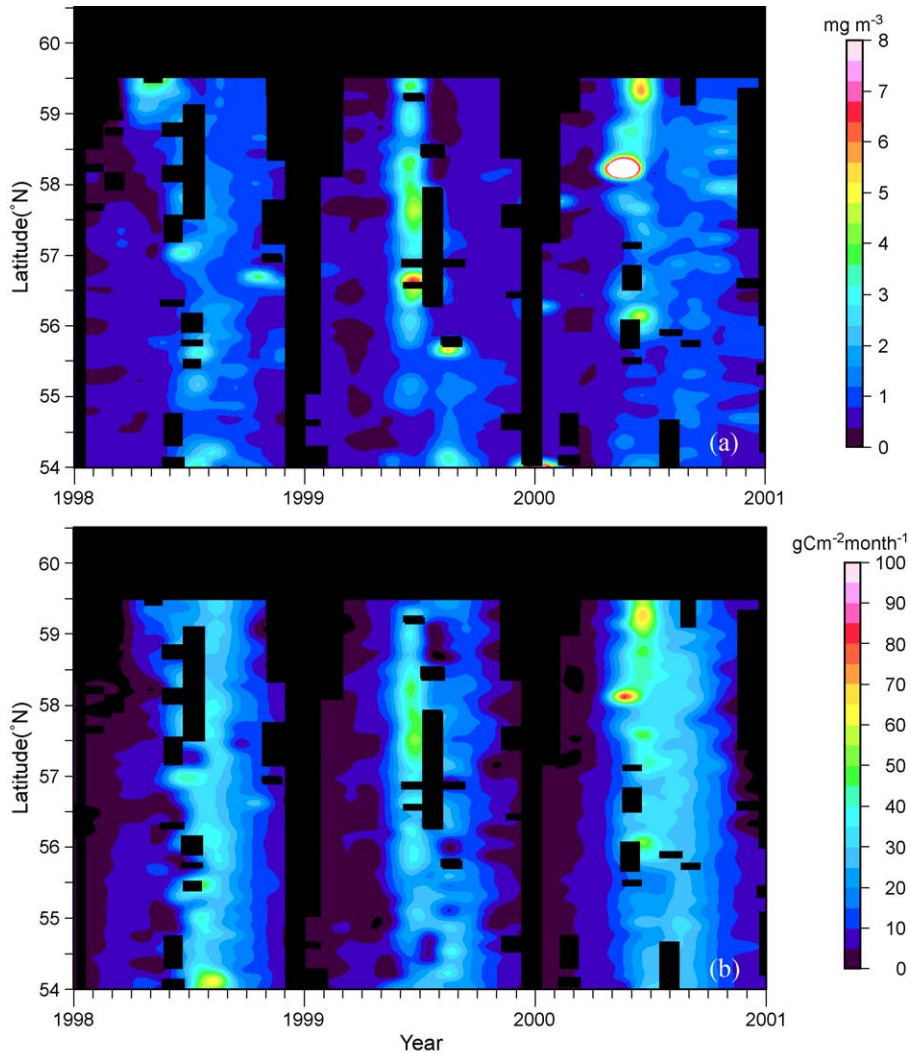


Fig. 5. Time–latitude plot of (a) chl-*a* concentration and (b) primary production using SeaWiFS chl-*a* and NOAA/AVHRR SST data directly under the ground track of TOPEX/Poseidon D-79. Black shade indicates cloud pixels. Primary production was calculated using the advanced VGPM (Behrenfeld and Falkowski, 1997) described by Kameda and Ishizaka (2004).

and Reed (1992) have argued that shoreward transport does not occur preferentially in the canyon, the horizontal mixing by mesoscale eddies could cause the capability of onshore transport of larval pollock and the oceanic zooplankton. In the summer of 1998, chl-*a* and primary production were relatively high (Fig. 5a and b) when SSHA RMS were high (Fig. 3b), implying that a strong horizontal current could cause the shelf–slope exchange. Conversely, relatively low eddy activity and stable conditions such as those ob-

served in the summer of 1999 generate a relatively unfertile environment. Over the Umnak Plateau, nutrient-rich water is transported along the Aleutian Arc by the inflow of Alaskan Stream through Amchitka Pass, Amukta Pass, and Unimak Pass (Schumacher and Reed, 1992; Stabeno et al., 1999), and plays an important role in maintaining the high productivity of this area, which had long periods of high chl-*a* and primary production around 54°N – 55°N (over the Umnak Plateau) even during the summer of 1999.

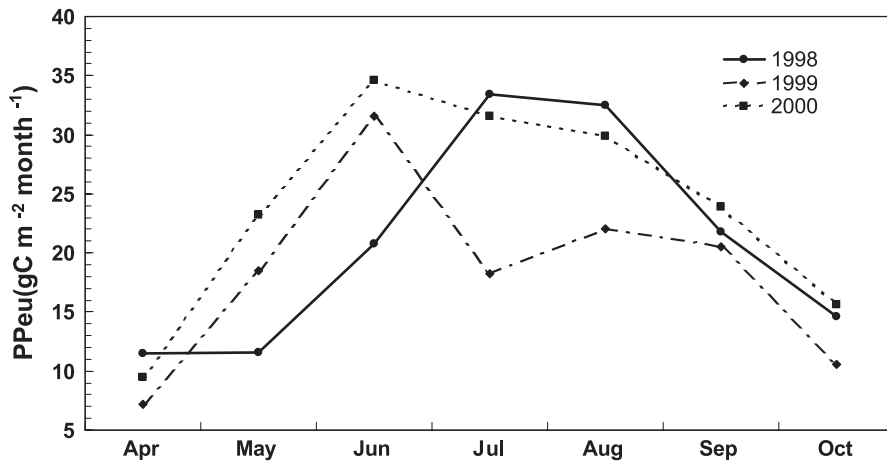


Fig. 6. Averaged primary production along the shelf edge from 1998 to 2001 estimated from SeaWiFS chl-*a*, PAR, and NOAA/AVHRR Pathfinder SST data.

Besides horizontal mixing, cyclonic and anticyclonic eddies generate upwelling of nutrient-rich water (Mizobata et al., 2002), therefore increasing the fluctuation of the eddy field contribution to the nitrogen transport into the euphotic zone following relatively high chl-*a* concentrations and horizontal mixing of low nutrient shelf water and high nutrient oceanic water (McRoy et al., 2001). In 2000, the eddy-rich environment along the shelf edge result maintained relatively high chl-*a* and primary production after the spring bloom. Generally, in the oceanic region, prey concentrations are low and are dominated by less preferred prey items, but mesoscale features, when present, may contain much higher prey densities, with a larger proportion of the prey types preferred by first-feeding larvae (Napp et al., 2000). Thus, the eddy-rich environment along the shelf break in 2000 might have provided a preferable environment for larval walleye pollock. However, the relationships between eddy activity and SeaWiFS chl-*a* are not coherent in the wintertime (TOPEX/Poseidon orbital cycles 225–245 and 260–280, after 300). In the winter, phytoplankton growth is light-limited rather than nitrogen-limited at the Bering Sea shelf edge and in the basin due to low solar insolation and strong winter convection. Consequently, the nutrient supply into the euphotic zone by mesoscale eddies will contribute little to phytoplankton growth in the wintertime. This is the reason why chl-*a* is often not coherent with eddy activity.

From time–latitude plots of D-79 SSHAs (Fig. 3a and b), we assume that the variability of the occurrence of mesoscale eddy was due to changes in BSC transport and speed. The speed of eddy propagation in 1998 and 1999 was slower than in 2000. This indicates that the physical conditions along the shelf edge in 1998 and 1999 were more stable and less likely to generate mesoscale eddies. Especially, in 1999, our analyses revealed small fluctuations in the eddy field and low speed of northwestward eddy propagation, indicating a decreased supply of eddy kinetic energy by the BSC.

The main source of the BSC with eddies is the Aleutian North Slope Current (ANSC), which flows eastward along the northern side of the Aleutian Islands resulting from the inflow of the Alaskan Stream through Amchitka Pass and Amukta Pass (Reed and Stabeno, 1999). The advection of the Alaskan Stream is strongly affected by Aleutian low pressure events (Hollowed and Wooster, 1992), and the sea level pressure (SLP) field in the northeastern North Pacific showed more intense winter Aleutian lows in 2000, as opposed to 1999, implying weak advection into the Alaskan Stream (not shown). Additionally, local wind forcing has little effect on ocean currents (Schumacher and Reed, 1992; Cokelet and Stabeno, 1997), and the strong variability of inflow through Amchitka Pass, Amukta Pass, and Unimak Pass was evident (Stabeno and Reed, 1994; Stabeno et al., 1999). Hence, the SLP field has indicated that there was relatively strong inflow of the Alaskan

Stream and the increasing transport of the ANSC and the BSC, leading to eddy-rich conditions along the shelf edge in 2000. From in situ observations, the transport in the ANSC and BSC systems (the reference level of 1500 dbar or the bottom) increased in 2000 (P.J. Stabeno, personal communication), which corresponded to our results. Although there is no evidence to explain the interaction among the Aleutian low pressure, ANSC, and BSC, the effects of climatic forcing on the current system around the Bering Sea and Gulf of Alaska deserve consideration.

The relationship of the Bering Slope Current eddy field and primary production was described using satellite multisensor remote sensing in this study. However, small-scale mesoscale features were neglected due to limited SSHAs and chl-*a*. In future work, we plan to conduct more high-resolution analyses that take into account small eddy activity.

Acknowledgements

We thank Dr. Richard D. Brodeur, Dr. Phyllis J. Stabeno, and an anonymous reviewer for their valued and constructive comments. We are grateful for the improvement of P_{opt}^B by Dr. Takuhiko Kameda and Dr. Joji Ishizaka. We also thank Dr. John R. Bower for reading through our manuscript and improving our English. Part of this study is supported by the National Space Development Agency of Japan (NASDA) through the program of Arctic Research projects using International Arctic Research Center (IARC)–NASDA Information System (INIS) and Satellite Data. Also this work was partly supported by Grant-in Aid (14405026) for Science Research from the Ministry of Education, Culture, Sports, Science, and Technology, Japan (S.S.). We appreciate all the help and support of the concerned research institutes, including the University of Alaska, Fairbanks and IARC. All figures were described using the Generic Mapping Tool (GMT) and SeaWiFS chl-*a* was processed using SeaDAS.

References

- Behrenfeld, M.J., Falkowski, P.G., 1997. Photosynthetic rates derived from satellite-based chlorophyll concentration. *Limnol. Oceanogr.* 42, 1–20.
- Benada, J.R., 1997. PO.DAAC Merged GDR (TOPEX/Poseidon) Generation B User's Handbook, Version 2.0, Jet Propulsion Laboratory, Pasadena, CA.
- Bograd, S.J., Stabeno, P.J., Schumacher, J.D., 1994. A census of mesoscale eddies in Shelikof Strait, Alaska, during 1989. *J. Geophys. Res.* 99, 18243–18254.
- Cokelet, E.D., Stabeno, P.J., 1997. Mooring observations of the thermal structure, salinity, and currents in the SE Bering Sea basin. *J. Geophys. Res.* 102, 22947–22964.
- Hollowed, A.B., Wooster, W.S., 1992. Variability of winter ocean conditions and strong year classes of Northeast Pacific ground fish. *ICES Mar. Sci. Symp.* 195, 433–444.
- Ince, L.S., Kendall Jr., A.W., Schumacher, J.D., Reed, R.K., 1991. Interactions of a mesoscale patch of larval fish (*Theragra chalcogramma*) with the Alaska Coastal Current. *Cont. Shelf Res.* 9, 269–284.
- Kameda, T., Ishizaka, J., 2004. Size-fractionated primary production estimated by two-phytoplankton community model. *J. Oceanogr.* (submitted for publication).
- Kinder, T.H., Coachman, L.K., Galt, J.A., 1975. The Bering Slope Current system. *J. Phys. Oceanogr.* 5, 231–244.
- Kinder, T.H., Schumacher, J.D., Hansen, D.V., 1980. Observation of a baroclinic eddy: an example of mesoscale variability in the Bering Sea. *J. Phys. Oceanogr.* 10, 1228–1245.
- Liu, H., Suzuki, K., Minami, C., Saino, T., Watanabe, M., 2002. Picoplankton community structure in the subarctic Pacific Ocean and the Bering Sea during summer 1999. *Mar. Ecol. Prog. Ser.* 237, 1–14.
- McRoy, C.P., Whitedge, T.E., Springer, A.M., Simpson, E.P., 2001. The nitrate front in the Bering Sea: is this an iron curtain? 2001 Aquatic Sciences Abstract CS10. <http://www.aslo.org/albuquerque2001/1097.html>.
- Mizobata, K., Saitoh, S., Shiimoto, S., Miyamura, T., Shiga, N., Toratani, M., Kajiwara, Y., Sasaoka, K., 2002. Bering Sea cyclonic and anticyclonic eddies observed during summer 2000 and 2001. *Prog. Oceanogr.* 55, 65–75.
- Napp, J.M., Kendall Jr., A.W., Schumacher, J.D., 2000. A synthesis of biological and physical processes affecting the feeding environment of larval walleye pollock (*Theragra chalcogramma*) in the eastern Bering Sea. *Fish. Oceanogr.* 9, 147–162.
- Okkonen, S.R., 1993. Observations of topographic planetary waves in the Bering Slope Current using the Geosat altimeter. *J. Geophys. Res.* 98, 22603–22613.
- Okkonen, S.R., 2001. Altimeter observations of the Bering Slope Current eddy field. *J. Geophys. Res.* 106, 2465–2476.
- Reed, R.K., Stabeno, P.J., 1999. The Aleutian North Slope Current. In: Loughlin, T.R., Ohtani, K. (Eds.), *Dynamics of the Bering Sea*. University of Alaska Sea Grant Press, Fairbanks, AK, pp. 177–191. AK-SG-99-03.
- Sapozhnikov, V.V., 1993. Influence of mesoscale anticyclonic eddies on the formation of hydrochemical structures in the Bering Sea. *Oceanology* 33, 299–304 (English translation).
- Schumacher, J.D., Reed, R.K., 1992. Characteristics of currents over the continental slope of the eastern Bering Sea. *J. Geophys. Res.* 97, 9423–9434.
- Schumacher, J.D., Stabeno, P.J., 1994. Ubiquitous eddies of the

- eastern Bering Sea and their coincidence with concentrations of larval pollock. *Fish. Oceanogr.* 3, 182–190.
- Schumacher, J.D., Stabeno, P.J., Bograd, S.J., 1993. Characteristics of an eddy over a continental shelf: Shelikof Strait, Alaska. *J. Geophys. Res.* 98, 8395–8404.
- Shiimoto, S., Saitoh, S., Imai, K., Toratani, M., Ishida, Y., Sasaoka, K., 2002. Interannual variation in phytoplankton biomass in the Bering Sea basin in the 1990s. *Prog. Oceanogr.* 55, 147–163.
- Springer, A.M., McRoy, C.P., Flint, M.V., 1996. The Bering Sea Green Belt: shelf edge processes and ecosystem production. *Fish. Oceanogr.* 5, 205–223.
- Stabeno, P.J., Meurs, V., 1999. Evidence of episodic on-shelf flow in the southeastern Bering Sea. *J. Geophys. Res.* 104, 29715–29720.
- Stabeno, P.J., Reed, R.K., 1994. Circulation in the Bering Sea basin observed by satellite-tracked drifters: 1986–1993. *J. Phys. Oceanogr.* 24, 848–854.
- Stabeno, P.J., Schumacher, J.D., Ohtani, K., 1999. The physical oceanography of the Bering Sea. In: Loughlin, T.R., Ohtani, K. (Eds.), *Dynamics of the Bering Sea*. University of Alaska Sea Grant Press, Fairbanks, AK, pp. 1–28. AK-SG-99-03.
- Sukhanova, I.N., Semina, J.H., Venttsel, M.V., 1999. Spatial distribution and temporal variability of phytoplankton in the Bering Sea. In: Loughlin, T.R., Ohtani, K. (Eds.), *Dynamics of the Bering Sea*. University of Alaska Sea Grant Press, Fairbanks, AK, pp. 453–483. AK-SG-99-03.